

# The effective S-matrix from conductance data in a quantum wave guide: Distinguishing the indistinguishable

Gursoy B. Akguç<sup>1</sup>, Jorge Flores<sup>1</sup>, and Sergey Yu. Kun<sup>1,2,3</sup>

<sup>1</sup>Centro de Ciencias Físicas,  
Universidad Nacional Autónoma de México,  
Cuernavaca, Morelos, México

<sup>2</sup>Center for Nonlinear Physics, RSP hysSE,  
The Australian National University,  
Canberra ACT 0200, Australia and

<sup>3</sup>Department of Theoretical Physics, RSP hysSE  
The Australian National University,  
Canberra ACT 0200, Australia

(Dated: April 14, 2024)

We consider two different stationary random processes whose probability distributions are very close and indistinguishable by standard tests for large but limited statistics. Yet we demonstrate that these processes can be reliably distinguished. The method is applied to analyze conductance fluctuations in coherent electron transport through nanostructures.

PACS numbers: 02.50.-r; 73.63-b

The quantum mechanical scattering by complex systems has been a problem of long-standing interest. This problem is of a great importance in nuclear, molecular and mesoscopic physics [1, 2, 3, 4]. The scattering process can be often analyzed in terms of two distinct time scales: (i) a prompt response due to direct processes and (ii) a time-delayed scattering mechanism. In nuclear physics the time-delayed mechanism is associated with the formation of an equilibrated compound nucleus [1, 5]. Similarly, time-delayed processes have been encountered in the study of coherent electron transport through nanostructures [1, 2, 3, 4, 6]. The two distinct time scales introduce two different energy scales. Namely, the scattering amplitude of direct processes is a smooth function of energy and it can be taken as an energy averaged S-matrix. The scattering amplitude of time-delayed process, on the other hand, is an energy dependent function which fluctuates rapidly around zero. Knowledge of the energy averaged S-matrix allows one to construct a probability distribution (PD) of the full S-matrix [6, 7, 8].

S-matrix for ballistic electron scattering on nanostructures can be calculated numerically if the geometry of the nanodevice, as well as the shape, size and number of propagating modes of the leads, and spatial distribution of disorder are known precisely. Then, having calculated the energy dependence of the S-matrix one can directly separate it into an energy averaged direct reaction component and a fluctuating one. In experiments, the detailed information about the conducting device may not be always available. For example, wall imperfections and unknown spatial distribution of disorder does not allow to evaluate the contribution of direct processes. Disorder can also block leads in an unknown manner reducing the number of propagating modes. This motivates us to consider the "inverse problem": What information about relative contributions of direct and time-delayed processes and number of propagating modes in the leads

can be obtained from the analysis of the transmission energy fluctuations provided the above mentioned characteristics of the nanodevice are unknown?

For concreteness we consider the transmission between horizontally oriented leads for the two types of geometry of wave guides (WG) (Fig. 1). For experimental purposes, we refer the reader to reference [9] for a possible implementation of this system. The left leads of both WG can accommodate a single propagating channel only. For the WG (b) the right lead also accommodates only one channel ( $N = 1$ ), while for WG (a) it has  $N = 2$  open channels. In addition, both WG (a) and (b) have  $N_a = 1$  and  $N_b = 1$  open channels shown by arrows pointing down at the bottom of WG with  $N_a = N$ . Disorder is modeled by scatterers (shown in Fig. 1 in white) having infinitely high potential walls.

Transmission between the horizontally oriented leads for the (a) and (b) WG in Fig. 1 is given by

$$T(E) = \sum_{j=1}^N |S_{1j}(E)|^2 \quad (1)$$

Here  $S_{1j}(E)$  are the S-matrix elements for scattering between left leads "1" and right leads  $j$ , and  $E$  is electron energy. For the WG (b) in Fig. 1 the sum (1) contain only a single term ( $N = 1$ ). We use the decomposition  $S_{1j}(E) = \langle S_{1j} \rangle + \delta S_{1j}(E)$ , where  $\langle S_{1j} \rangle$  are energy averaged S-matrix elements, and  $\delta S_{1j}(E)$  are energy fluctuating ones. We choose the spacial distribution of disorder such that (i)  $\sum_j \langle S_{1j} \rangle^2 = 1$ , and (ii) transmission between the horizontal leads and open channels at the bottom of both (a) and (b) WG in Fig. 1 is mostly due to time-delayed processes. Therefore, the overall amount of direct processes for the transmission between different channels is much less than that for the overall amount of time-delayed processes. Also, due to the presence of disorder, the dynamics of the classical

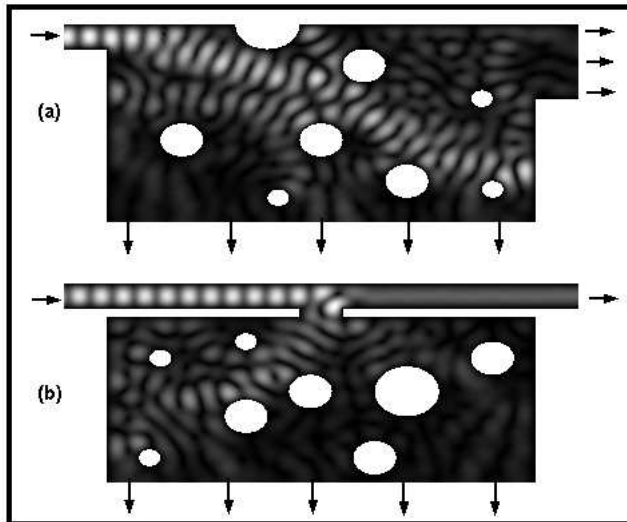


FIG. 1: The electron probability distribution inside the wave guides for an arbitrary chosen electron energy. The arrows show incident unit current from left and current leaving the system from the right. The white circular regions represent finite potential barriers. The wave guide (a) does not show direct processes and (b) has direct processes (see text).

counterpart in the interaction region of WG (a) and (b) in Fig. 1 is chaotic. Since the total numbers of open channels,  $N + N_a + 1$  and  $N + 2$ , are much greater than unity, we are in the regime of Ericson fluctuations when electron resonance states within the WG are overlapping. Then each individual fluctuating S-matrix element can be considered as a Gaussian random process. Namely, real and imaginary parts of each individual  $S_{1j}(E)$  in sum (1) are distributed by a Gaussian law, are uncorrelated and have the same dispersions [1, 5].

The PD for  $y = T(E) = \langle T(E) \rangle$  (so that  $\langle y \rangle = 1$ ) is given by [5],

$$P_N(y) = N (1 - y_d)^{-1} (y - y_d)^{N-1} \exp[-N(y + y_d)(1 - y_d)] I_{N-1}[2N(y - y_d)^{1/2}(1 - y_d)^{1/2}]: \quad (2)$$

Here  $I_{N-1}(\cdot)$  is the modified Bessel function of  $(N-1)$  order and  $y_d = \sum_j |S_{1j}|^2 / \sum_j \langle |S_{1j}|^2 \rangle = \langle T(E) \rangle$  is the relative contribution of direct processes to the total transmission. The PD of Eq. (2) is exact if all  $S_{1j}(E)$  with different  $j$  are uncorrelated and have the same dispersions. Otherwise this PD is an approximation for which  $N$  should be understood as an effective number of independent channels  $N_{eff} < N$ . It is given by the normalized variance of  $T(E) = \sum_{j=1}^N |S_{1j}(E)|^2$ :  $\langle T(E)^2 \rangle / \langle T(E) \rangle^2 - 1 = 1/N_{eff}$ .

For the WG (b) in Fig. 1 one has to put  $N = 1$  in Eq. (2). For  $y_d = 0$ , Eq. (2) takes the form of a  $\chi^2$ -distribution with  $2N$  degrees of freedom [5]:

$$P_N(y) = N [N!]^{-1} (Ny)^{N-1} \exp(-Ny); \quad (3)$$

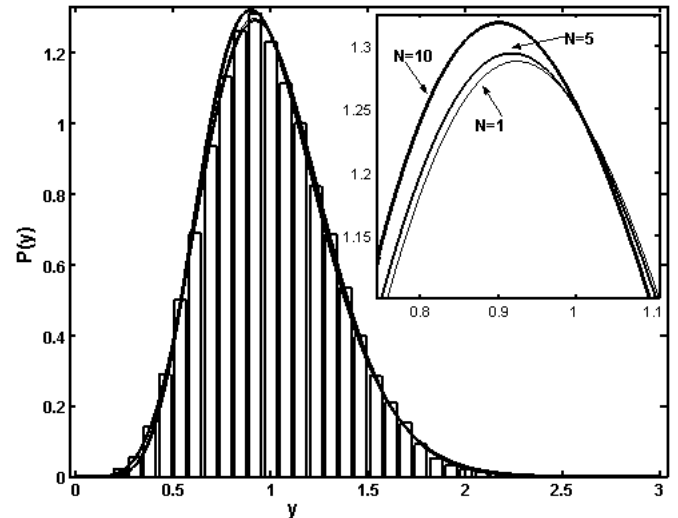


FIG. 2: The probability distributions of transmission. The solid lines, with decreasing thicknesses, show the theoretical curves for  $N = 1$ ,  $N = 5$  (Eq. (2)) and  $N = 10$  (Eq. (3)) channel cases respectively. The histogram is constructed from the numerical data for  $N = 1$  and  $y_d = (0.9)^{1/2}$ , as an example. The inset shows a blow up of the transmission probability distributions demonstrating that the difference between them around their maximum does not exceed 4%.

where  $J_N(\cdot)$  is Gamma function. Note that the variance of  $y$  is given by  $\langle y^2 \rangle - 1 = (1 - y_d^2)/N$  [5].

As an example, we consider two possible cases for WG (a) in Fig. 1: (i)  $N = 10$  and  $y_d = 0$ , the latter due to complete blocking of the direct paths between the leads by disorder, and (ii)  $N = 5$  and  $y_d = (0.9)^{1/2}$ . Also suppose that, for WG (b), for which  $N = 1$ ,  $y_d = (0.9)^{1/2}$ . For the above three sets of  $N$  and  $y_d$  values the variance of conductance  $y$  is the same and equals 0.1. The question is: Can we distinguish these three cases by analyzing PD of  $y$  in Eq. (2)?

In Fig. 2 we plot the PD for the three sets of  $N$  and  $y_d$ . The three distributions are very close. We performed a  $\chi^2$  test and found that, even for as many as 28000 independent realizations of  $y$  for each of the three cases, the distributions are indistinguishable at a 99% confidence level. And, to the best of our knowledge, there is currently no any other statistical test which would allow to distinguish between the three different stochastic processes. Yet, in what follows, we show that the problem of distinguishing between these random processes can be solved.

We will refer to the  $y$  as  $y_i$ , where the index  $i$  stands for different independent realizations of the process. Let us transform to new random variables  $s_{ij} = (y_i + y_j)/2$ ,  $r_{ij} = (y_i - y_j)/2 = 2s_{ij}$  with  $i \neq j$ . One can now easily find the joint probability distribution  $K(s;r)$ . The analytical calculations are formally similar to those of Ref. [10] for the analysis of the correlation between cross section and analyzing power in the regime of Ericson fluctuations in

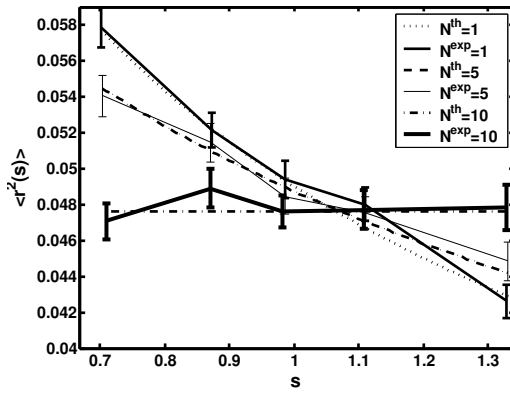


FIG. 3: The plot of  $\langle r^2(s) \rangle$  vs.  $s$  corresponding to the same  $N$  (shown in inset) and  $y_d$  values as those used for the analysis of the probability distributions in Fig. 2. Dotted, dashed and dotted-dashed lines are theoretical predictions (Eq. (4)).

nuclear reactions. Without presenting the explicit result for  $K(s;r)$  we point out that, for  $y_d = 0$ ,  $s$  and  $r$  are statistically independent. On the contrary, for  $y_d \neq 0$ ,  $s$  and  $r$  correlate, the bigger  $y_d$  the stronger this correlation is.

We calculate  $\langle r^2(s) \rangle$ :

$$\langle r^2(s) \rangle = [1 - \mathbb{E}_{N+3}(\cdot) - \mathbb{E}_{2N-1}(\cdot)] / (2N+1); \quad (4)$$

where  $\mathbb{E} = 4N(y_d s)^{1-2} = (1 - y_d)$ , and take into account the constraint  $(1 - y_d) = N = 0:1$ . In Fig. 3, we show  $\langle r^2(s) \rangle$  for the three cases. We have generated 28000 realizations for each case and used all possible  $i < j$  combinations for  $s_{ij}$  and  $r_{ij}$ . The data in Fig. 3 are obtained by dividing the  $s_{ij}$  into 5 bins for each case and taking the average of  $r^2(s)$  and  $s$  for each bin. It is evident from Fig. 3 that we can distinguish the three cases. The fluctuations around the theoretical curves are determined by the number of realizations. Error bars are calculated numerically from standard deviations of 100 data sets each consisting 28000  $y$  realizations. We found that it is possible to distinguish the  $N = 1$  and  $N = 10$  processes in 97% of cases for 210 realizations of  $y$ . This drops to 85% for 140 realizations.

We apply the new method to distinguish between (a) and (b) in Fig. 1 from the conductance fluctuation data. We implemented a finite element solution of the Schrodinger equation [9, 11]. Calculations were performed on the energy range which allows 5 propagating channels in the right lead for WG (a) in Fig. 1. Both left leads for WG (a) and (b) as well as the right lead for WG (b) in Fig. 1 accommodate a single channel. In addition, for both (a) and (b) WG in Fig. 1, there are 20-25 propagating channels from the lower part of the devices. A unit current is directed from left. We are interested in the transmission probability from the left to the right side. Spatial disorder distribution for WG (a) in Fig. 1 was chosen to block the direct paths between the left and

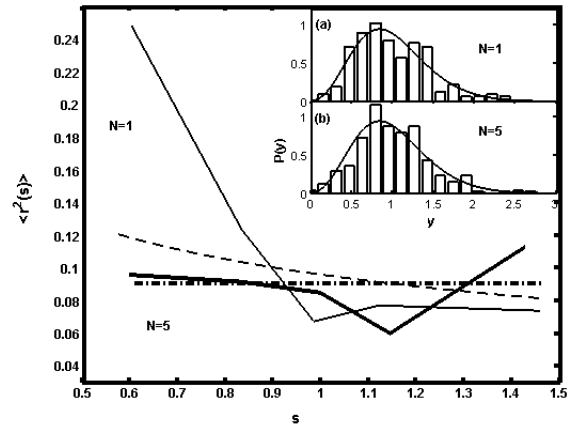


FIG. 4: The plot of  $\langle r^2(s) \rangle$  vs.  $s$  for the wave guides shown in Fig. 1. The dashed and dotted-dashed lines are theoretical estimates (Eq. (4)) and thin and thick solid lines are numerical calculations for  $N = 1$  (with direct processes) and for  $N = 5$  (without direct processes) cases respectively. The inset shows conductance distributions (lines) for (a)  $N = 1$ , with direct processes (Eq. (2)), and (b)  $N = 5$ , without direct processes (Eq. (3)). Histograms are constructed from the numerical data.

right leads, i.e. to maximally suppress direct processes. This was confirmed by S-matrix numerical data, which yielded negligible absolute value of the energy averaged S-matrix, and by the fact that the normalized variance of conductance fluctuations is close to 0.2. For WG (b) in Fig. 1 the extension of leads into the cavity is adjusted to have relative contribution of direct process  $y_d = 0.9$  so that the normalized variance of conductance fluctuations is close to 0.2, i.e. to that for WG (a) in Fig. 1. For both (a) and (b) WG in Fig. 1 we used different disorder distributions to increase the statistics. The overall number of independent realizations of transmission values  $y$  for each type of geometry in Fig. 1 was around 150.

In Fig. 4 we present PD of  $y$  for the (a) and (b) WG of Fig. 1.  $\chi^2$  test does not allow to distinguish the two PD. Yet, from Fig. 4 one can see that for the  $N = 1$  case, in the presence of direct processes,  $\langle r^2(s) \rangle$  strongly increases when  $s$  decreases. On the contrary, for the  $N = 5$  case, when direct processes are absent,  $\langle r^2(s) \rangle$  for  $s < 1$  is close to a constant. We have checked that even for each single configuration of disorder, when we have only about 30-40 independent realizations of the transmission values for each (a) and (b) WG,  $\langle r^2(s) \rangle$  increases always noticeably faster for the  $N = 1$  case with direct processes as compared to the  $N = 5$  case without direct processes. On the other hand, the rise of  $\langle r^2(s) \rangle$  when  $s$  decreases of  $s$  for  $N = 1$  with direct processes is much stronger than that predicted by Eq. (4). In order to find a possible reason for this we analyzed the PD of fluctuating S-matrix elements. We found that (i)  $S_{11}(E)$  are not distributed isotropically in the complex plane, (ii) the PD of real and imaginary parts of  $S_{11}(E)$

are not Gaussian, and (iii) real and imaginary parts of  $S_{11}(E)$  are correlated. Therefore, the reason for the discrepancy between the data and theoretical line in Fig. 4 for  $N = 1$  is that the conditions to derive Eq. (4) are not met. Yet, the distribution for transmission is not sensitive to the deviation of the PD of  $S_{11}(E)$  from its isotropic Gaussian distribution in the complex plane and correlation between real and imaginary parts of  $S_{11}(E)$ .

In conclusion, we have suggested a method to distinguish between different stationary random processes

whose PD are very close and indistinguishable by standard tests for large but limited statistics. The method has been applied to analyze conductance fluctuations in coherent electron transport through WG. We found that the method proposed here, unlike the analysis of PD of transmission, is sensitive to (i) the deviation of PD of fluctuating transmission amplitudes from isotropic Gaussian statistics in the complex plane, and (ii) correlations between real and imaginary parts of the fluctuating transmission amplitudes.

- 
- [1] T. Guhr, A. Müller-Groeling and H.A. Weidenmüller, Phys. Rep. 299, 189 (1998), and references therein.
- [2] C.W.J. Beenakker, Rev. Mod. Phys. 69, 731 (1997), and references therein.
- [3] Y. Alhassid, Rev. Mod. Phys. 72, 895 (2000).
- [4] Jonathan P. Bird, J. Phys.: Condens. Matter 11, R413 (1999).
- [5] T. Ericson and T. Mayer-Kuckuk, Ann. Rev. Nucl. Sci. 16, 183 (1966), and references therein.
- [6] Gursoy B. Akçuc and L.E. Reichl, Phys. Rev. E 67, 046202, 2003.
- [7] P.A. Melby, P. Pereyra, and T.H. Seligman, Ann. of Phys. 161, 254 (1985); W.A. Friedman and P.A. Melby, *ibid.* 161, 276 (1985).
- [8] V.A. Gopar and P.A. Melby, Eur. Phys. Lett. 42, 131 (1998).
- [9] Gursoy Akçuc, Linda Reichl, Anil Shaji and Michael Snyder, Phys. Rev. A 69, 042303 (2004).
- [10] S.Yu. Kun, Z. Phys. A 321, 165 (1985).
- [11] Gursoy B. Akçuc and L. Reichl, J. Stat. Phys. 98, 813 (2000).